Finate amplitude bed deformations in totally and partially transporting wide channel bends

(Article begins on next page)

Finite amplitude bed deformations in totally and partially transporting wide channel bends

G. Seminara and L. Solari

Istituto di Idraulica, Università di Genova, Genova, Italy

Abstract. We develop an analytic approach able to predict flow and bed topography in curved cohesionless wide channels. The novel feature of the present theory, compared with previous analytic approaches, is its ability to treat bottom perturbations of finite amplitude and situations such that sediment transport does not occur within the whole cross section. The theory is presently applied to the case of constant curvature channels though it can be extended, in principle, to channels with variable curvature. Results show that the dominant mechanism controlling the establishment of bed profile is the topographic feedback of bottom deformations on the flow field, while the role of the dispersive transverse transport of longitudinal momentum and of the metrically induced transverse variations of longitudinal slope is usually relatively small. The theory extends previous linear analyses which are shown to underpredict deeping of the cross section close to the outer bank. Also, unlike linear theories, the present approach predicts a transverse slope of the bed profile increasing towards the outer bend in agreement with experimental observations. The maximum depth is found to depend on the friction coefficient C_u of the undisturbed uniform stream and on the parameter $\nu(\theta_u)^{1/2}/C_u$ where ν is curvature ratio, that is, the ratio between channel half width and radius of curvature of the centerline, while θ_u is the Shields stress of the undisturbed uniform stream. Comparison with experimental observations is fairly satisfactory. The shape of the cross section is then determined also for values of θ_u close enough to the critical values not to allow bedload transport within the whole cross section. The threshold value of θ_u separating the total transport from the partial transport regime is finally determined as a function of the curvature ratio ν.

1. Introduction

Investigations on the subject of bed topography in curved cohesionless channels have been proposed by several authors in the last two decades (for a recent review see the AGU monograph *River Meandering* [*Ikeda and Parker*, 1989]). The various approaches appeared so far in the literature may roughly be classified into two main groups: (1) linear and weakly nonlinear theories which are essentially based on the assumption that perturbations of bottom elevation associated with the effect of curvature are sufficiently small compared with the unperturbed flow depth [*Blondeaux and Seminara*, 1985; *Johannesson and Parker*, 1989; *Seminara and Tubino*, 1992] and (2) strongly nonlinear numerical calculations which remove the latter restrictions at the expense of some numerical effort [e.g., *Smith and McLean*, 1984; *Struiksma et al.*, 1986; *Nelson and Smith*, 1989; *Colombini and Tubino*, 1990; *Shimizu et al.*, 1990].

The advantage of theoretical analyses over numerical approaches is usually their ability to provide insight on the basic mechanisms operating in the process under investigation. On the other hand, numerical work is usually superior in that it allows removal of the restrictions of linearity or weak nonlinearity which may severely reduce the range of applicability of theoretical approaches.

The importance of analytical work is also related to the need to provide to engineers simple tools (like formulas or plots) able to predict the scour depth developing in river bends under given hydraulic conditions. In fact, it is astonishing how little of the recent research achievements in the field of river morphodynamics is actually used by designers of bank protection works. For instance, the latest version of the *U.S. Army Corps of Engineers* [1991] manual covering the subject of bank protection is based only on poorly correlated field observations relating scour depth at the outer bank to channel curvature.

In the present paper we investigate the possibility of relaxing the linear assumption in the context of an analytic approach as long as flow and bottom topography may be described as "slowly varying" in both planimetric directions and curvature effects are small enough. The former assumption essentially requires the channel to be "wide" with width and channel alignment varying on a longitudinal scale much larger than channel width, while the latter assumption is satisfied provided a typical measure of the radius of curvature of flow streamlines (say the radius of curvature of channel axis) is large compared with flow depth. Both conditions are indeed satisfied in actual rivers but notice that neither of them implies that perturbations of bottom topography are necessarily small.

In order to check the feasibility of the above idea we start our analysis considering the simplest possible case of channels with constant width and constant curvature. Restricting our investigation to the fully developed region of the flow, where longitudinal variations of flow and bottom characteristics vanish, we are led to revisit a classical problem which has been
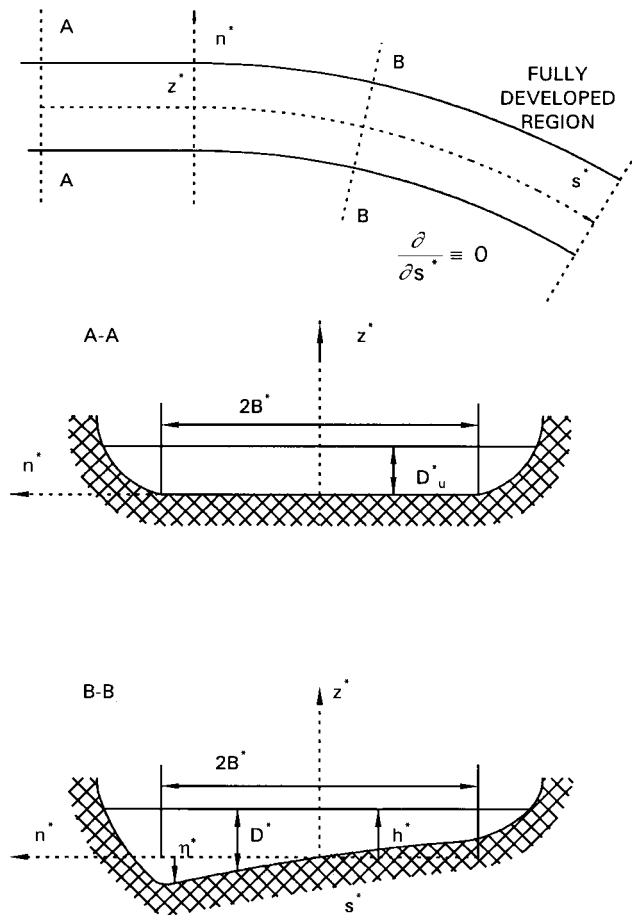
Figure 1. Sketch and notation.

analyzed by several authors in the past, starting from the pioneering contribution of *Rozovskij* [1957].

The basic novel idea pursued herein may be summarized as follows. Let the unknown finite perturbations of bottom topography be described by some unknown function of the planimetric coordinates. Then the flow field may be evaluated at the leading order of approximation as a slowly varying sequence of locally uniform flows driven by the local characteristics (unknown flow depth and shear velocity) slightly perturbed by a weak curvature-induced secondary flow. The whole solution may hence be expressed analytically in terms of the unknown function describing the distribution of bottom topography. The latter function is finally obtained as the solution of a differential equation found by imposing the requirement of sediment continuity along with the integral constraint whereby flow discharge is assigned.

It will appear that a further, usually ignored condition must be satisfied, namely, the requirement that under steady conditions, sediment flow rate must also be constant. We show that in order for such a condition to be satisfied, the longitudinal slope of a channel with constant curvature must be slightly smaller than that associated with an equivalent straight reach. Such an observation, which plays a minor role for uniform sediments, is found to be crucially important in the case of heterogeneous sediments [*Seminara et al.*, 1997].

The advantage of the present approach is that it allows physical insight, is relatively simple, and can deal with finite

scour even in the context of flow conditions such that sediment transport can not occur along the whole cross section.

The procedure employed in the rest of the paper is as follows. In the next section we formulate the mathematical problem of flow and sediment motion in constant curvature wide cohesionless channels with dominant bed load transport. This problem is then solved in the fully developed region (section 3). The case of partially transporting cross sections is tackled in section 4. Results and comparison with previous (linear) theories and experimental observations are discussed in section 5. Some conclusions follow in section 6.

2. Formulation of the Problem

We consider a wide curved cohesionless channel, characterized by constant curvature of channel axis and departing from a straight reach (Figure 1).

Let us refer the flow field to orthogonal curvilinear coordinates s^*, n^*, z^* (hereafter a superscript asterisk will denote a dimensional quantity subsequently made dimensionless). Notice that s^* denotes a longitudinal coordinate defined along the channel axis, n^* is a transverse coordinate spanning the cross section, and z^* is a nearly vertical coordinate orthogonal to the plane (s^*, n^*) and pointing upwards.

We assume the channel axis to be a circular helix characterized by a constant value of the radius of curvature r_o^*. Furthermore, we set

$$\cos \theta_s \simeq 1 \tag{1}$$

where θ_s is the angle that the tangent to the channel axis forms with a horizontal plane.

The metric coefficients of the above coordinate system are readily found to read

$$h_s = 1 + \frac{n^*}{r_o^*} \quad h_n = 1 \quad h_z = 1 \tag{2}$$

Let us then consider the steady and fully developed flow of a constant discharge Q in the curved reach. The fully developed character of the flow field and of bottom topography is mathematically described by the condition that derivatives $\partial f/\partial s^*$, with f any function describing a property of either the flow field or bed topography, must identically vanish. Experimental observations suggest that fully developed conditions are indeed reached in constant curvature channels at a sufficient distance downstream from the entrance. In the experiments of *Kikkawa et al.* [1976] such a distance was roughly 6.5 channel widths. Let S_u be the constant slope of the channel axis in the straight reach preceding the bend under investigation and denote by U_u^*, D_u^*, and C_u the average speed, flow depth, and friction coefficient characterizing the uniform flow of the constant discharge Q in such a straight reach. The reader should notice that S_u does not coincide with the slope of the bottom in the fully developed region of the bend (S_d). The reason for such difference will become clear in the course of the analysis.

We then define dimensionless quantities as follows:

$$(U^*, V^*, W^*) = U_u^*(U, V, W) \tag{3a}$$

$$P^* = (\varrho U_u^{*2})P \tag{3b}$$

$$(z^*) = D_u^*(z) \tag{3c}$$

$$(s^*, n^*) = B^*(s, n) \tag{3d}$$

$$\nu_T^* = (\sqrt{C_u}U_u^*D_u^*)\nu_T \qquad (3e)$$

$$q_n^* = q_n\sqrt{(s-1)gd_s^{*3}} \qquad (3f)$$

where (U, V, W) is the local velocity vector averaged over turbulence (U longitudinal, V transverse, W vertical components), P is the mean pressure, ν_T is the local value of an eddy viscosity, q_n is the transverse component of the bed load discharge vector, and d_s^* and s, are respectively, diameter and relative density of sediments taken to be uniform.

Having set the above notation, we can write the governing equations for the fluid and the sediments in the following dimensionless form:

$$V_{,n} + \nu h_s^{-1}V + \beta W_{,z} = 0 \qquad (4a)$$

$$\beta\sqrt{C_u}[\nu_T U_{,z}]_{,z} = (h_s^{-1}P_{,s} - h_s^{-1}C_u\beta) + VU_{,n}$$
$$+ \beta WU_{,z} + \nu h_s^{-1}UV \qquad (4b)$$

$$\beta\sqrt{C_u}[\nu_T V_{,z}]_{,z} = P_{,n} - \nu h_s^{-1}U^2 + VV_{,n} + \beta WV_{,z} \qquad (4c)$$

$$P_{,z} = -\frac{1}{F_u^2} \qquad (4d)$$

$$q_{n,n} + \nu h_s^{-1}q_n = 0 \qquad (4e)$$

where a comma preceding a subscript denotes partial differentiation with respect to the corresponding spatial coordinate. Notice that longitudinal derivatives have been set equal to zero in the continuity equation for the fluid (equation (4a)) and for the sediments (equation (4e)) as well as in the Reynolds equations (equations (4b)–(4d)). Furthermore, only the effect of the dominant components of Reynolds stresses (T_{zs} and T_{zn}) has been retained in (4b) and (4c). Various dimensionless parameters appear in the governing differential system, namely, the Froude number F_u, the half width to depth ratio β, the curvature ratio ν, and the friction coefficient C_u. They are defined in the following form:

$$F_u = \frac{U_u^*}{\sqrt{gD_u^*}} \qquad (5a)$$

$$\beta = \frac{B^*}{D_u^*} \qquad (5b)$$

$$\nu = \frac{B^*}{r_o^*} \qquad (5c)$$

$$C_u^{-1/2} = 6 + 2.5\ln\frac{D_u^*}{2.5d_s^*} \qquad (5d)$$

having estimated the absolute bottom roughness as equal to $2.5\,d_s^*$.

In the following we will assume the channel to be "wide" and "weakly curved"; hence we write

$$\beta \gg 1 \qquad (6a)$$

$$\nu \ll 1 \qquad (6b)$$

Assumption (6a) allows us to ignore the role of the side walls concentrating our attention on the central region of the flow. The latter does not interact strongly with the side wall boundary layers at least under natural conditions due to the relatively low slope of natural banks. Assumption (6b) will allow us to treat the flow field as slightly perturbed with respect to the flow

in a straight channel. However it will appear that such procedure does not imply that bottom topography is only slightly perturbed relative to a flat configuration.

The differential problem (4a)–(4e) will be solved subject to the following boundary conditions:

$$U = V = W = 0 \qquad z = z_0(n) \qquad (7a)$$

$$P = U_{,z} = V_{,z} = W - \frac{V}{\beta}\frac{\partial h}{\partial n} = 0 \qquad z = h(n) \qquad (7b)$$

$$q_n = 0 \qquad (n \pm 1) \qquad (7c)$$

In condition (7a), $z_0(n)$ denotes the local value of the conventional reference level for no-slip scaled by D_u^*. Condition (7b) imposes the restriction that the stress vanishes at the free surface which is a material surface, $h(n)$ being the local value of free surface elevation (scaled by D_u^*) and having approximated the z axis with the vertical axis. Finally, condition (7c) expresses the requirement that the side walls must be impermeable to sediments.

In order to close the problem we must introduce convenient closure assumptions for ν_T and $\mathbf{q}$.

We take advantage of the slowly varying character of the flow field and bottom topography which derives from the assumption that the channel is wide and the flow is fully developed. As a result we assume that the turbulent structure is in a condition of quasi-equilibrium whereby the flow field may be interpreted as a sequence of uniform states in equilibrium with the local conditions only slightly perturbed by the effect of curvature. Hence, recalling that under uniform conditions the eddy viscosity is proportional to the local values of friction velocity and flow depth and, for given slope of the free surface, friction velocity is proportional to the square root of flow depth, we write

$$\nu_T = \left(\frac{|\boldsymbol{\tau}^*|}{\varrho C_u U_u^{*2}}\right)^{1/2}D(n)N(\zeta) \qquad (8)$$

in which $\boldsymbol{\tau}$ is tangential stress vector at the bottom, $D(n)$ is local value of the dimensionless flow depth, and ζ is a normalized vertical coordinate which maps the actual cross section into the rectangle

$$\zeta_0 \leq \zeta \leq 1 \qquad -1 \leq n \leq 1 \qquad (9)$$

The definition of ζ reads

$$\zeta = 1 + \frac{z - h(n)}{D(n)} \qquad (10)$$

The vertical distribution of eddy viscosity $N(\zeta)$ is taken to coincide with that characteristic of uniform flow. We write

$$N(\zeta) = \frac{k\zeta(1-\zeta)}{1 + 2A\zeta^2 + 3B\zeta^3} \qquad (11)$$

in which k is von Karman's constant and A, B values are those adopted by *Dean* [1974] for his wake function ($A = 1.84$, $B = -1.56$).

Sediment transport will be assumed to occur dominantly as bed load. Its direction deviates from the direction of bottom stress because of the effect of gravity, which in the present case of constant curvature channel and fully developed flow acts in the transverse direction. The deviation angle plays a crucial role, and its evaluation has been the subject of several theoretical and experimental investigations, among the most recent

of which are the works of *Kovacs and Parker* [1994] and *Talmon et al.* [1995]. In particular, the output of the latter experimental study confirms that a reasonable structure for q_n reads

$$q_n = \left[\frac{\tau_n}{|\tau|} - \frac{r}{\beta\sqrt{\theta}} \frac{\partial(h-D)}{\partial n} \right] \phi(\theta) \tag{12}$$

where r is an empirical constant which ranges about 0.6 and ϕ is the uniform bed load function for which several semiempirical formulas are available in the literature, θ being the local value of Shields stress defined as

$$\theta = \frac{|\tau^*|}{(\varrho_s - \varrho)gd_s^*} \tag{13}$$

The problem formulated above is subject to two integral constraints. The first stipulates that the upstream value of fluid discharge must be constant along the curved reach; hence in dimensionless form,

$$\int_{-1}^{1} D \, dn \int_{\zeta_0}^{1} U(\zeta, n) \, d\zeta = 2 \tag{14}$$

The second constraint imposes a similar condition on sediment discharge and reads

$$\int_{-1}^{1} \phi[\theta(n)] \, dn = 2\phi_u(\theta_u) \tag{15}$$

in which θ_u and ϕ_u are the values of Shields stress and bed load function in the straight reach, respectively.

3. Solution for the Case of Totally Transporting Cross Section

We seek a solution of the problem formulated in section 2, based on a perturbation expansion different from that commonly employed in previous analysis [e.g., *Seminara and Tubino*, 1989].

The crucial idea is that of relaxing the assumption of "small amplitude" perturbations of flow and bottom topography relative to the classical solution of uniform flow in a straight channel. Indeed, even in a weakly curved channel the local scour at the outer bend may be found to be of the order of the average flow depth, and similarly the perturbations of longitudinal flow driven by such distortions of bottom topography are of finite amplitude. However, we wish to show that relaxing the latter assumption does not preclude the possibility of obtaining a simple analytic solution of the problem. In fact, we may take advantage of the fact that the channel is wide and weakly curved to expand the solution in a neighbourhood of the solution for the flow in a straight channel with unknown shape of the bottom profile, described by some unknown function $D(n)$, which becomes the major output of the analysis.

In the present case, channel curvature being constant in the longitudinal direction, the secondary flow is only driven by the local unbalance between transverse pressure gradient and centrifugal force. Equation (4c) shows that the actual parameter measuring the magnitude of secondary flow is $(\nu/\beta(C_u)^{1/2})$. Hence we denote the latter parameter by δ and set the following expansion:

$$(U, V, W, P, h, D) = (U_0(\zeta, n), 0, 0, P_0(\zeta, n), 1, D_0(n))$$

$$+ \delta\left(U_1, V_1, \frac{W_1}{\beta}, P_1, h_1, D_1 \right)$$

$$+ \delta^2\left(U_2, V_2, \frac{W_2}{\beta}, P_2, h_2, D_2 \right) + O(\delta^3) \tag{16a}$$

where

$$\delta = \frac{\nu}{\beta\sqrt{C_u}} \tag{16b}$$

Notice that the further rescaling of W appearing in (16a) is suggested by the equation of flow continuity (4a).

Substituting from (16a) into (4a)–(4e); (7a)–(7c) and (8); and (10)–(15) and using the chain rules

$$\frac{\partial}{\partial z} \to \frac{1}{D} \frac{\partial}{\partial \zeta} \tag{17a}$$

$$\frac{\partial}{\partial n} \to \frac{\partial}{\partial n} + \left[(1-\zeta) \frac{D_{,n}}{D} - \frac{h_{,n}}{D} \right] \frac{\partial}{\partial \zeta} \tag{17b}$$

we equate likewise powers of (δ) to obtain a sequence of problems at the various orders of approximation.

3.1. Leading Order: Uniform Flow in a Straight Channel With Unknown Cross-Sectional Shape

At the leading order of approximation $O(\delta^0)$ the z component of Reynolds equations, along with boundary condition (7b), gives

$$P_{0,\zeta} = -\frac{D_0}{F_u^2} \tag{18a}$$

$$P_0|_{\zeta=1} = 0 \tag{18b}$$

hence

$$P_0 = \frac{D_0}{F_u^2}(1-\zeta) \tag{18c}$$

The latter result simply states a well known fact, namely, that pressure is hydrostatically distributed in a uniform open channel flow.

Similarly, the s component of Reynolds equations at leading order describes uniform flow in a straight channel with the unknown transverse distribution of flow depth $D_0(n)$. We find

$$U_0 = D_0^{1/2}(n)\mathscr{F}_0(\zeta, n) \tag{19a}$$

with

$$[N(\zeta)\mathscr{F}_{0,\zeta}]_{,\zeta} = -\sqrt{C_u} \tag{19b}$$

$$\mathscr{F}_0|_{\zeta=\zeta_0} = \mathscr{F}_{0,\zeta}|_{\zeta=1} = 0 \tag{19c}$$

and, recalling (11), the solution for $\mathscr{F}(\zeta, n)$ reads

$$\mathscr{F}_0 = \frac{\sqrt{C_u}}{k} \left[\ln \frac{\zeta}{\zeta_0(n)} + A\zeta^2 + B\zeta^3 \right] \tag{20}$$

where $\zeta_0(n)$ is the normalized form of the conventional reference level for no slip and reads

$$\zeta_0 = \frac{\zeta_u}{D_0(n)} \tag{21a}$$

$$\zeta_u = \exp\left(-\frac{k}{\sqrt{C_u}} - 0.777 \right) \tag{21b}$$

The solution (19a)–(19c), (20), (21a), and (21b) shows that at the leading order of approximation, the longitudinal component of fluid velocity exhibits the classical logarithmic distribution corrected by a wake function. However, notice that the unknown shape of the cross section affects the amplitude of U_0, which is proportional to the 1/2 power of local flow depth. Also notice that the vertical distribution $\mathcal{F}_0$ is weakly dependent on the transverse coordinate n through the effect of transverse variations of relative roughness associated with the (finite) transverse variations of flow depth (see (21a)).

3.2. First Order: Curvature-Induced Fully Developed Secondary Flow and Finite Scour in Constant Curvature Channels

Let us proceed to $O(\delta)$. At this order the n component of the momentum equations can be solved along with the equation of continuity to give the leading-order approximation of the secondary flow.

Equation (4c) suggests setting

$$\frac{dh_1}{dn} = F_u^2 a_1(n) D_0(n) \tag{22a}$$

$$V_1 = D_0^{3/2}(n)\mathcal{G}_1(\zeta, n) \tag{22b}$$

in which $\mathcal{G}_1$ is the solution of the following differential problem

$$[N(\zeta)\mathcal{G}_{1,\zeta}]_{,\zeta} = a_1(n) - \mathcal{F}_0^2(\zeta, n) \tag{23}$$

$$\mathcal{G}_1|_{\zeta=\zeta_0} = \mathcal{G}_{1,\zeta}|_{\zeta=1} = 0 \tag{24}$$

Notice that the structure (22b) of the solution for the transverse component of velocity implies that the intensity of the secondary flow increases in the outward direction because of the factor $D_0^{3/2}$, while the vertical distribution of V_1 varies slightly as predicted by the solution of the differential problem (23) and (24).

The latter variations are forced by the weak dependence of the centrifugal acceleration on the transverse coordinate, resulting from the transverse variations of relative roughness affecting $\mathcal{F}_0$. On the other hand, the transverse slope of the free surface increases in the outward direction as predicted by (22a).

In the context of linear theories neither V_1 nor dh_1/dn vary in the transverse direction.

The differential problem (24) is readily solved numerically in terms of the unknown function $a_1(n)$. We find that

$$\mathcal{G}_1 = a_1(n)\left[g_1(\zeta; n) - \frac{g_1'|_{\zeta=1}}{g_0'|_{\zeta=1}} g_0(\zeta; n) \right]$$

$$+ g_2(\zeta; n) - \frac{g_2'|_{\zeta=1}}{g_0'|_{\zeta=1}} g_0(\zeta; n) \tag{25}$$

with $g_i(i = 1, 2, 3)$ being the solution of the following differential systems

$$\frac{d}{d\zeta}\left[N \frac{dg_i}{d\zeta} \right] = \delta_i \quad g_i|_{\zeta_0} = 0 \quad g_i'|_{\zeta_0} = 1 \qquad i = 0, 1, 2 \tag{26}$$

where

$$\delta_0 = 0 \quad \delta_1 = 1 \quad \delta_2 = -\mathcal{F}_0^2(\zeta, n) \tag{27}$$

In order to evaluate the quantity $a(n)$ we need to impose an integral condition arising from the equation of continuity. In

fact, by integrating (4a) from the bottom to the free surface we find

$$W_1 = -D_0'D_0^{3/2}\left[\mathcal{G}_1(1 - \zeta) + \frac{5}{2}\int_{\zeta_0}^{\zeta} G_1(\zeta', n)\, d\zeta' \right]$$

$$- D_0^{5/2}\int_{\zeta_0}^{\zeta} \frac{\partial G_1}{\partial n}\, d\zeta' \tag{28}$$

But recalling (7b), at leading order we require that $W_1|_{\zeta=1}$ must vanish; hence (28) gives

$$\int_{\zeta_0}^{1} G_1(\zeta, n)\, d\zeta = 0 \tag{29}$$

Using (25), (29) finally gives

$$a_1(n) = -\frac{I_{g_2} - (g_2'|_1/g_0'|_1)I_{g_0}}{I_{g_1} - (g_1'|_1/g_0'|_1)I_{g_0}} \tag{30}$$

having employed

$$I_f = \int_{\zeta_0}^{1} f\, d\zeta \tag{31}$$

Finally, we proceed to determine the unknown function $D_0(n)$ by solving the sediment continuity equation, which at leading order imposes that the transverse component of sediment flow rate must vanish everywhere in the cross section. Hence we find

$$\frac{dD_0}{dn} = d_0(n)D_0^{3/2} \tag{32}$$

where

$$d_0 = -\frac{\nu\sqrt{\theta_u}}{r\sqrt{C_u}}\frac{\mathcal{G}_{1,\zeta}|_{\zeta_0}}{\mathcal{F}_{0,\zeta}|_{\zeta_0}} = \bar{d}_0[a_1(n) - I_{\mathcal{F}_0^2}] \tag{33}$$

in which θ_u is the Shields stress of the uniform flow in a straight reach with slope S_u and $\bar{d}_0$ is the following parameter:

$$\bar{d}_0 = \frac{\nu\sqrt{\theta_u}}{C_u r} \tag{34}$$

In (34), r, the empirical constant, is defined in (12). From (32)–(34) two interesting observations arise:

1. The transverse slope of the bottom is an increasing function of the transverse coordinate, which is in agreement with all experimental observations.

2. The amplitude of bottom perturbations is controlled by the parameter $\bar{d}_0$; hence scour increases linearly with curvature and with the square root of Shields stress. Notice that $\bar{d}_0$, the actual parameter controlling the intensity of bottom scour, typically ranges between 0 and few tenths, and the maximum scour may be a finite quantity in spite of the fact that curvature is small.

Unfortunately, (32) cannot be solved analytically, as d_0 depends weakly on the transverse coordinate through the functions $\mathcal{F}_0$ and $\mathcal{G}_1$ (see (33)). Furthermore, the solution of (32) is to be obtained subject to the integral constraint (14), which at leading order gives

$$\int_{-1}^{1} D_0^{3/2} \, dn \int_{\zeta_0}^{1} \mathscr{F}_0(\zeta, n) \, d\zeta = 2 \qquad (35)$$

Hence (32) can only be solved numerically by a trial and error procedure, that is, by varying the initial condition for $D_0|_{n=-1}$ until constraint (35) is satisfied.

Finally, notice that in order for condition (15) to be satisfied, the bottom slope must gradually change from the straight reach to the fully developed curved reach in order to accommodate a constant sediment discharge along with the finite deformations of the bottom profile. This observation does not seem to have been pointed out before.

3.3. First Order: Correction of Longitudinal Motion due to the Metric Variation of Bottom Slope and of the (Transverse and Vertical) Transport of Longitudinal Momentum

In a constant curvature channel the bottom slope varies in the transverse direction because of metric variations of the longitudinal coordinate. Moreover, our leading-order solution for the longitudinal velocity was simply a uniform flow solution slowly varying in the transverse direction. However, because of the effect of the curvature-induced secondary flow, longitudinal momentum is transported outward close to the free surface and inward close to the bed.

As a result of such transverse variation of bottom slope and transverse transport of longitudinal momentum, an $O(\delta)$ perturbation of longitudinal velocity is then produced. In fact, by perturbing (8) one obtains

$$\nu_T = \nu_{T_0}\left[1 + \left(\frac{D_1}{D_0} + \frac{U_{1,\zeta}}{U_{0,\zeta}}\bigg|_{\zeta_0}\right)\delta + O(\delta^2)\right] \qquad (36)$$

Hence some algebra allows us to show that the problem for U_1 reads

$$[N(\zeta)U_{1,\zeta}]_{,\zeta} - [N(\zeta)U_{1,\zeta}]_{\zeta_0} = \sqrt{C_u}D_0^{1/2}\left[n\beta\sqrt{C_u} - \frac{D_1}{D_0}\right]$$

$$+ \frac{W_1}{\beta\sqrt{C_u}}\frac{d\mathscr{F}_0}{d\zeta} + \frac{D_{0,n}D_0^{3/2}}{\beta\sqrt{C_u}}\left[\frac{1}{2}\mathscr{G}_1\mathscr{F}_0 + (1-\zeta)\mathscr{G}_1\frac{d\mathscr{F}_0}{d\zeta}\right]$$

$$+ \frac{D_0^{3/2}}{\beta\kappa}D_{0,n}\mathscr{G}_1 \qquad (37a)$$

$$U_{1,\zeta}|_{\zeta=1} = 0 \qquad (37b)$$

$$U_1|_{\zeta=\zeta_0} = 0 \qquad (37c)$$

The latter problem is immediately solved. It is convenient to set

$$U_1 = D_0^{1/2}\mathscr{F}_1(\zeta, n) \qquad (38)$$

where

$$\mathscr{F}_1 = \frac{D_{0,n}D_0}{\beta\sqrt{C_u}}\left[f_1(\zeta, n) - \frac{f_1'}{f_0'}\bigg|_{\zeta=1} f_0(\zeta, n)\right]$$

$$- \frac{D_0^2}{\beta\sqrt{C_u}}\left[f_2(\zeta, n) - \frac{f_2'}{f_0'}\bigg|_{\zeta=1} f_0\right] \qquad (39)$$

and $f_i(\zeta; n)$ $(i = 0, 1, 2)$ satisfy the following problems:

$$[N(\zeta)f_{i,\zeta}]_{,\zeta} = \phi_i(\zeta; n) \qquad (40a)$$

$$f_i|_{\zeta_0} = 0 \qquad (40b)$$

$$f_{i,\zeta}|_{\zeta_0} = 1 \qquad (40c)$$

$$f_{i,\zeta\zeta}|_{\zeta_0} = f_{1,\zeta}|_{\zeta_0}\left(1 - \frac{N'}{N}\bigg|_{\zeta_0}\right) + \frac{\sqrt{C_u}}{k\zeta_0}\left(n\beta\sqrt{C_u} - \frac{D_1}{D_0}\right) \qquad (40d)$$

with

$$\phi_0 = 0 \qquad (41)$$

$$\phi_1 = \frac{1}{2}(\mathscr{G}_1\mathscr{F}_0)_{,\zeta} + \frac{\sqrt{C_u}}{\kappa}\mathscr{G}_{1,\zeta} - \frac{5}{2}\mathscr{F}_{0,\zeta\zeta}\int_{\zeta_0}^{\zeta}G_1(\zeta', n)\,d\zeta'$$

$$- \frac{5}{2}\mathscr{F}_{0,\zeta}\frac{\partial}{\partial\zeta}\int_{\zeta_0}^{\zeta}G_1(\zeta', n)\,d\zeta' \qquad (42)$$

$$\phi_2 = \mathscr{F}_{0,\zeta\zeta}\frac{\partial}{\partial n}\int_{\zeta_0}^{\zeta}G_1(\zeta', n)\,d\zeta' + \mathscr{F}_{0,\zeta}\frac{\partial^2}{\partial\zeta\partial n}\int_{\zeta_0}^{\zeta}G_1(\zeta', n)\,d\zeta' \qquad (43)$$

Notice that f_0 reads

$$f_0 = \left[(3B + 2A)(\zeta_0 - \zeta) + \ln\left(\frac{\zeta}{\zeta_0}\right) - \frac{3}{2}B(\zeta^2 - \zeta_0^2)\right]\zeta_0 \quad (44)$$

3.4. Second Order: Correction of Secondary Flow Driven by Inertia and by Corrections of Centrifugal Effects

Many second-order effects arise in the equation governing the secondary flow. Indeed, the $O(\delta)$ correction of longitudinal velocity affects the centrifugal term which also exhibits an $O(\delta^2)$ contribution associated with the metric transverse variation of curvature. Further contributions are due to the transverse variations of the transverse component of momentum, to topographic effects, and to perturbations of the eddy viscosity forced by perturbations of flow depth and longitudinal velocity.

Finally, notice that a correction of the transverse slope of the free surface must also be allowed for in order to satisfy the zero transverse flux condition at second order.

The solution for $h_2(n)$ and $V_2(\zeta, n)$ can conveniently be written in the form

$$\frac{dh_2}{dn} = \beta\sqrt{C_u}F_u^2 a_2(n)D_0(n) \qquad (45)$$

$$V_2 = D_0^{3/2}(n)G_2(\zeta, n) \qquad (46)$$

In substituting from (45) and (46) into (4c), (7a), and (7b) some algebra allows us to derive the differential problem for $G_2(\zeta, n)$ in the form

$$[NG_{2,\zeta}]_{,\zeta} = \Gamma_0(\zeta, n) \qquad (47)$$

$$G_2|_{\zeta_0} = 0 \qquad (48)$$

$$G_{2,\zeta}|_1 = 0 \qquad (49)$$

$$\Gamma_0(\zeta, n) = \left(\frac{D_1}{D_0} - \frac{\mathscr{F}_{1,\zeta}}{\mathscr{F}_{0,\zeta}}\bigg|_{\zeta_0}\right)[a_1(n) - \mathscr{F}_0^2]$$

$$+ a_2(n) - 2\mathscr{F}_0\mathscr{F}_1 + \beta\sqrt{C_u}n\mathscr{F}_0^2$$

$$+ \frac{1}{\beta\sqrt{C_u}}\left\{D_0^2\left(G_1G_{1,n} - G_{1,\zeta}\int_{\zeta_0}^{\zeta}G_{1,n}\,d\zeta'\right)\right.$$

$$\left. + D_0D_{0,n}\left(\frac{3}{2}G_1^2 - \frac{5}{2}G_{1,\zeta}\int_{\zeta_0}^{\zeta}G_1\,d\zeta'\right)\right\} \qquad (50)$$
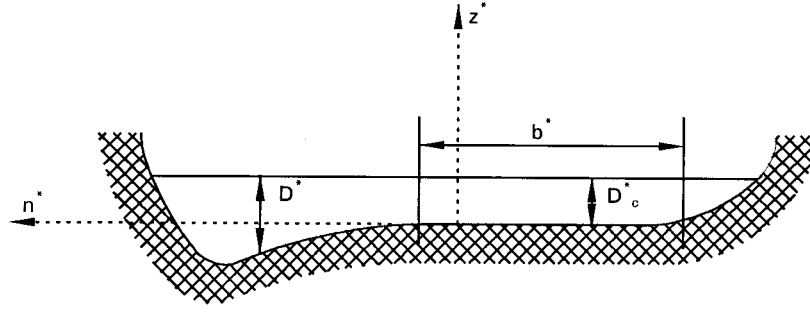
Figure 2. Sketch of a partially transporting cross section and notation.

The latter system can be solved in a way similar to that employed to evaluate G_1. Hence

$$G_2 = a_2(n) \left[g_1(\zeta, n) - \frac{g_1'|_{\zeta=1}}{g_0'|_{\zeta=1}} g_0(\zeta, n) \right]$$

$$+ g_{22}(\zeta, n) - \frac{g_{22}'|_{\zeta=1}}{g_0'|_{\zeta=1}} g_0(\zeta, n) \qquad (51)$$

where

$$[N g_{22,\zeta}]_{,\zeta} = \Gamma_2 \qquad (52)$$

$$g_{22}|_{\zeta_0} = 0 \qquad (53)$$

$$g_{22,\zeta}|_{\zeta_0} = 1 \qquad (54)$$

and

$$\Gamma_2 = \Gamma_0 - a_2(n) \qquad (55)$$

The unknown function $a_2(n)$ is then obtained by imposing that $G_2(\zeta, n)$ satisfies the integral condition arising from the continuity equation, namely,

$$\int_{\zeta_0}^1 G_2(\zeta, n) \, d\zeta = 0 \qquad (56)$$

Hence

$$a_2(n) = - \frac{Ig_{22} - \dfrac{g_{22}'|_{\zeta=1}}{g_0'|_{\zeta=1}} Ig_0}{Ig_1 - \dfrac{g_1'|_{\zeta=1}}{g_0'|_{\zeta=1}} Ig_0} \qquad (57)$$

Having determined U_1 and V_2, we may proceed to evaluate the $O(\delta)$ component of D_1.

In fact, sediment continuity requires that the $O(\delta^2)$ correction of the transverse component of bedload transport rate must also vanish. Since

$$\left. \frac{\tau_n}{|\boldsymbol{\tau}|} \right|_{\zeta=\zeta_0} = \delta \left. \frac{V_{1,\zeta}}{U_{0,\zeta}} \right|_{\zeta_0} + \delta^2 \left[\left. \frac{V_{2,\zeta}}{U_{0,\zeta}} \right|_{\zeta_0} - \left. \frac{V_{1,\zeta} U_{1,\zeta}}{U_{0,\zeta}} \right|_{\zeta_0} \right] + O(\delta^3) \quad (58)$$

$$\sqrt{\theta} = \sqrt{\theta_0} \left[1 + \delta \left. \frac{U_{1,\zeta}}{U_{0,\zeta}} \right|_{\zeta_0} + O(\delta^2) \right] \qquad (59)$$

from (12) we find

$$\frac{dD_1}{dn} = -\bar{d}_0 D_0^{3/2} \frac{G_{2,\zeta}|_{\zeta_0}}{\mathcal{F}_{0,\zeta}|_{\zeta_0}} \sqrt{C_u} \qquad (60)$$

The solution of (60) is obtained numerically with the help of the integral constraint (14), which at $O(\delta)$ gives

$$\int_{-1}^1 I_{\mathcal{F}_1} D_0^{3/2} \, dn = -\int_{-1}^1 I_{\mathcal{F}_0} D_0^{1/2} D_1 \, dn \qquad (61)$$

Also notice that the further integral constraint (15) can be satisfied only by allowing for an $O(\delta)$ correction of bottom slope.

4. Extension to the Case of Partially Transporting Cross Sections

As already mentioned, the problem formulated in section 3 has to be solved by a trial and error procedure. At leading order one starts from some initial distribution for $D_0(n)$ which allows one to calculate $\mathcal{F}_0$, $\mathcal{G}_1$, and W_1 by (20), (25), and (28), hence $d_0(n)$ from (33) and $D_0(n)$ by solving (32). Such procedure is repeated until the function $D_0(n)$ is such that the integral constraint (35) is satisfied with sufficient accuracy. A similar trial and error procedure is implemented to evaluate $D_1(n)$.

The latter procedure fails when the value of θ_u is so small that because of the deposition process occurring at the inner bend, within part of the cross section the water becomes so shallow as to reach the threshold conditions for sediment transport.

In the latter case the fully developed shape of the cross section takes the form depicted in Figure 2. For $-1 \leq n \leq b$ the flow depth takes the value D_c^* such that

$$\theta_c = \frac{\tau^*}{(\varrho_s - \varrho) g d_s^*} = \frac{\varrho g D_c^* S_d}{(\varrho_s - \varrho) g d_s^*} = D_c S_d \frac{\theta_u}{S_u} \qquad (62)$$

and hence

$$D_c = \frac{\theta_c}{\theta_u} \frac{S_u}{S_d} \qquad (63)$$

The trial and error procedure is then similar to that previously described except for the starting point of the calculation, which is located at $n = b$, with parameter b to be determined such that the integral constraint (35) is satisfied.

5. Results

Before we discuss the main results we point out that the differential systems for g_0, g_1, g_2, f_0, f_1, f_2, and g_{22} were solved numerically using a Runge-Kutta scheme of fourth or-
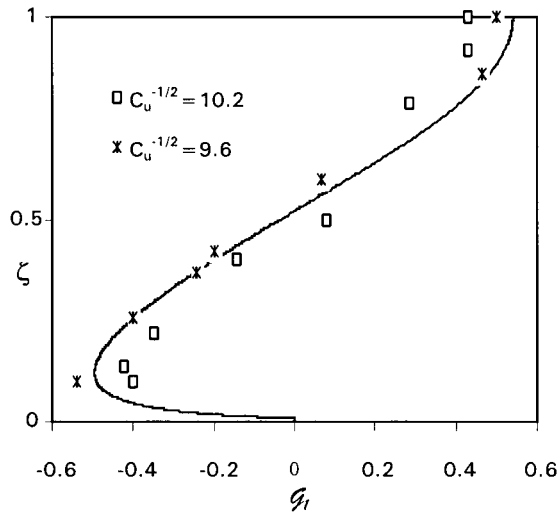
Figure 3. Comparison between the vertical distribution of the leading order transverse component of flow velocity according to the present theory (line) and the experimental results of *Rozovskij* [1957, run 8] (squares, asterisks).

der with 1000 steps after redefining the vertical coordinate in the form $\chi = \ln(\zeta/\zeta_0)$. Quadratures were performed using Simpson's rule.

The vertical distribution of secondary flow predicted by the present model varies weakly in the transverse direction be-

cause of variations in relative roughness. However, in the particular case of fixed bed ($D = 1$), the distribution keeps constant. Figure 3 shows a comparison between our theoretical predictions, which apply to the case of rough walls, and the classical experimental observations of *Rozovskij* [1957] (run 8; $s^* = (3/8)\pi r_o$). In the fixed bed case the structure of $\mathcal{G}_1(\zeta)$ obtained by our approach does not differ significantly from that of *de Vriend* [1977]; hence the latter comparison is equally satisfactory.

A comparison between our theoretical results for the transverse bed profile and the experimental observations (experiments 1 and 2) of *Kikkawa et al.* [1976] is given in Figure 4. Various sources of relative uncertainty are present in such comparison. First, in these series of experiments, migrating alternate (free) bars were present along with the forced bar associated with curvature, which is the subject of the present investigation. Second, the assumption of wide cross sections employed in the present analysis, quite suitable to natural channels, is only approximately satisfied by the experimental conditions set up by the above authors. In particular, the channel banks were vertical in the experiments, which implies that the effective width of the cross section practically unaffected by the presence of the side walls was slightly smaller than the actual width of the channel. Finally, the data reported in the papers were not sufficiently detailed to appreciate whether a difference between the upstream value of S_u and its downstream value S_d was observed.

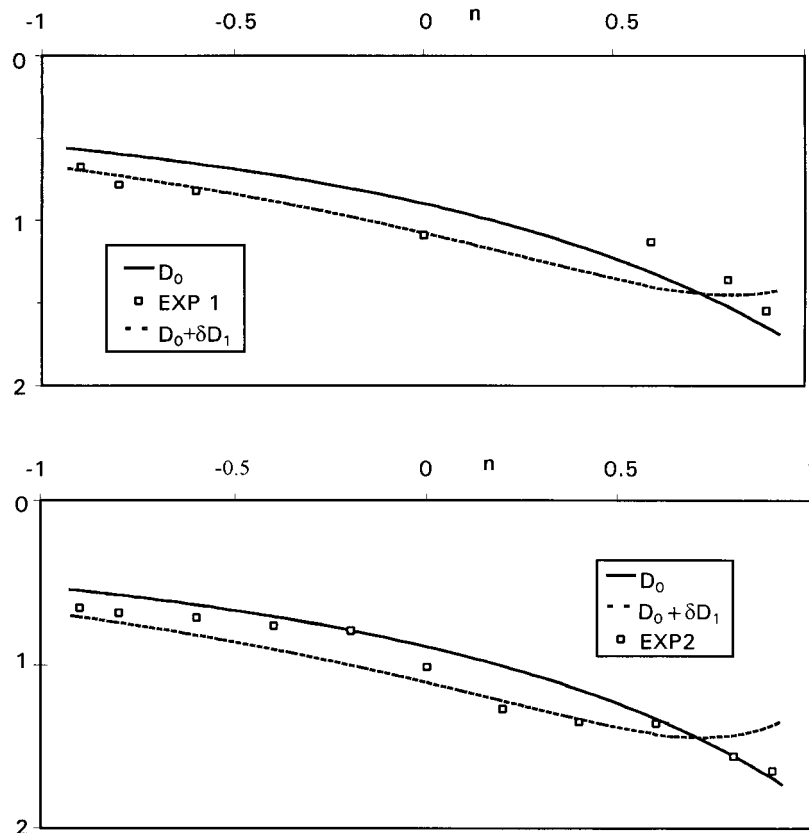The above concerns were taken care of as follows. The

Figure 4. Comparison between the bed profile predicted by the present theory (leading order, solid line; leading order plus first order, dashed line) and the experimental data of *Kikkawa et al.* [1976]. The value of the empirical parameter r employed was 0.6.

presence of alternate bars was averaged out by the above authors. Though the coexistence of free and forced bars may give rise to nonlinear interactions [*Tubino and Seminara*, 1990], we have assumed that data reported by the above authors refer to only the effects of forced bars. The relatively narrow character of the cross sections was accounted for by applying our theory to effective cross sections, treated as infinitely wide, and such that under uniform flow conditions, they carry the same discharge as the actual channel with a transversely uniform distribution of longitudinal velocity. The effective width of such channel ($2B_e^*$) was related to the actual width ($2B^*$) by the following relationship:

$$\frac{B^*}{B_e^*} = \left(1 + \frac{D_u^*}{B^*}\right)^{2/3} \qquad (64)$$

Formula (64) is based on assuming that the roughness of side walls is identical to that of the bottom. This is not the case in the experiments of *Kikkawa et al.* [1976]. However, it does not seem appropriate to refine the above correction, as its effect is fairly small. The agreement between theoretical findings and experimental data is satisfactory as it appears from Figures 4. A better agreement might be achieved by extending the analysis to also include the effect of the side wall boundary layers.

The maximum dimensionless flow depth predicted by the present theory is expressed by the following relationship

$$D|_{n=1} = D_0|_{n=1} + \left(\frac{\nu}{\beta\sqrt{C_u}}\right) D_1|_{n=1} + h.o.t. \qquad (65)$$

The dependence of the quantities $D_0|_{n=1}$ and $D_1|_{n=1}$ on the parameters $\bar{d}_0$ and C_u is represented in Figures 5 and 6, respectively. Figure 5 also shows the same dependence as predicted by the linear theory of *Seminara and Tubino* [1989]. Notice that the curve obtained by the present nonlinear theory merges into the linear curve as the parameter $\bar{d}_0$ defined by (34) tends to zero. Furthermore nonlinear predictions for the maximum depth significantly exceed the linear values for large values of $\bar{d}_0$ and/or C_u, while maximum deposition is overestimated by the linear approach.

Figures 7 and 8 show the first order corrections for the longitudinal and transverse components of the flow velocity. Such corrections are found to be sufficiently small compared with the leading-order approximations. These results suggest
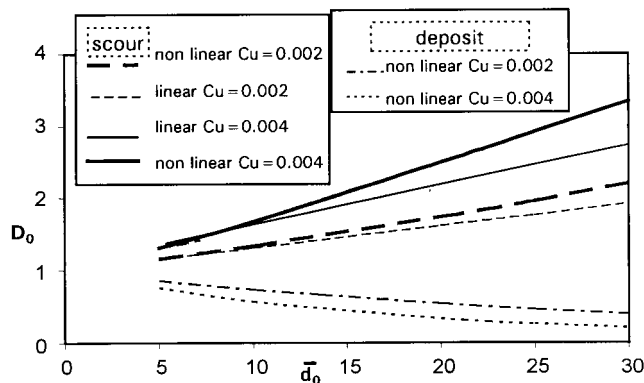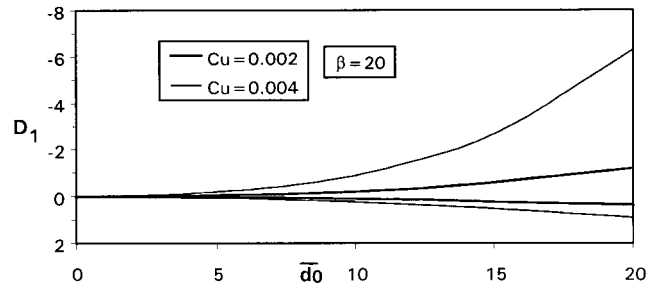

Figure 6. Maximum scour and maximum deposit predicted by the present theory at the first order.

that the assumed perturbation procedure is rational. Also notice that U_1 is negative both at the inner and at the outer portions of the cross section. This finding has a simple physical explanation. The $O(\delta)$ correction for U is driven by three major effects: (1) the transverse transport of longitudinal momentum, which tends to decelerate the outer flow and accelerate the inner flow; (2) the metric decrease of channel slope in the outward direction; and (3) the topographic effect associated with $O(\delta)$ perturbations of bottom topography, which Figure 6 shows to be negative in the outer bend and positive in the inner bend.

Hence each of effects 1–3 leads to acceleration at the inner bend and deceleration of the outer flow.

Notice that the change of curvature of the bottom profile induced, close to the outer bend, by the $O(\delta)$ correction for D is a consequence of the negative value of U_1 throughout the cross section. Indeed, in order for the $O(\delta)$ correction of flow discharge to vanish, with U_1 negative definite, D_1 must change sign somewhere within the cross section. This result appears to be interesting, as it may allow easy matching between the side wall boundary layers and the flow in the central region investigated herein.

Finite amplitude scour of the outer bend arises from a self-sustaining mechanism: An increasing finite distortion of the bed profile gives rise at leading order to an increasing amplitude of both longitudinal and secondary flow (respectively proportional to $D_0^{1/2}$ and $D_0^{3/2}$), which in turn require an increasing transverse bed slope to achieve equilibrium. In other words, the topographic feedback of bottom deformations on the flow field appears to be the dominant mechanism controlling the establishment of bottom topography, while the role of the transverse dispersive transport of longitudinal momentum is relatively minor, as is that of the metrically induced transverse variations of longitudinal slope. However, Figure 6 shows that for large values of $\bar{d}_0$ and/or C_u, the $O(\delta)$ correction for D increases very fast, leading to failure of the perturbation scheme. Fortunately, as it appears from the definition of $\bar{d}_0$, increasing the value of C_u also leads to decreasing $\bar{d}_0$, which suggests that the above failure will seldom occur.

Figure 9 shows that the downstream slope S_d slightly differs from its upstream value S_u, the less so as the undisturbed value of Shields stress increases for given $\bar{d}_0$ and/or C_u decreases. Notice that *Parker*'s [1990] transport formula was employed in Figure 9 to evaluate the bed load function $\phi(\theta)$, though quite similar results have been obtained using the Meyer-Peter transport formula.

The fact that S_d is different from S_u is physically obvious: indeed, bed load transport is nonlinearly related to Shields stress. Hence the increase of transport due to an increase of
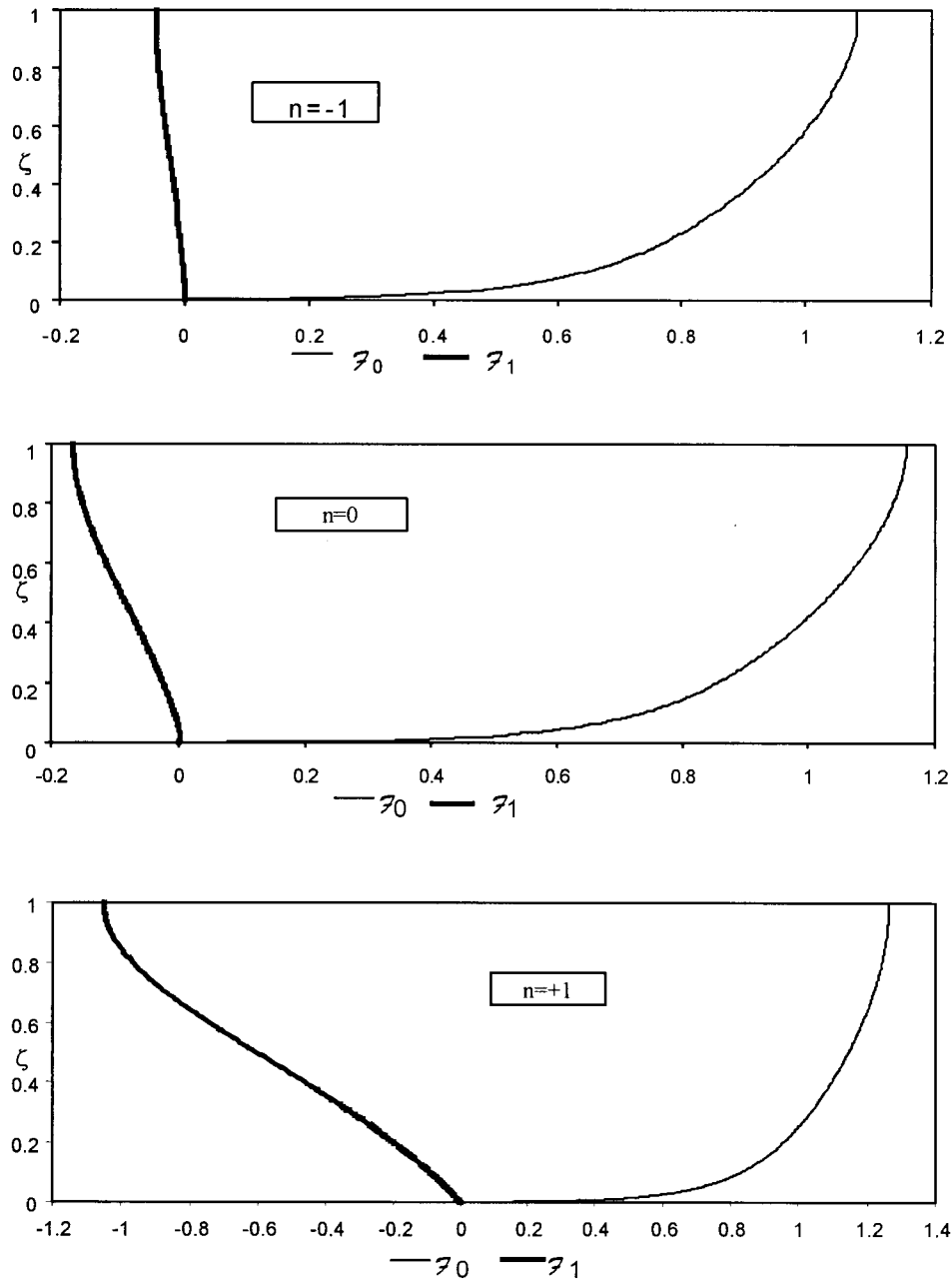

Figure 5. Maximum scour (solid and dashed lines) and maximum deposit (dashed-dotted and dotted lines) predicted by the present theory at the leading order. The linear prediction for the maximum scour obtained by *Seminara and Tubino* [1989] is also shown.

Figure 7. Typical vertical distribution of longitudinal velocity at $n = 0, 1, -1$ at leading order $\mathcal{F}_0$ (thin line) and first order $\mathcal{F}_1$ (thick line). Parameter values are $C_u = 0.004$, $\beta = 20$.

flow depth in the outer portion of the cross section exceeds the reduction of transport associated with decreasing the flow depth in the inner region. In order to balance this effect, such to keep the total transport constant, the downstream channel slope must decrease.

At last, let us provide some results concerning the case of partially transporting cross sections. Figure 10 shows the length b of the inactive part of the channel scaled by half width as a function of θ_u/θ_c for a given value of C_u and two different values of $\bar{d}_0$. Obviously, the whole channel width is inactive when θ_u is less than or equal to θ_c. As θ_u exceeds θ_c a portion of the channel width becomes active and, as expected, for given $\theta_u > \theta_c$ the active length increases as the parameter $\bar{d}_0$ decreases. Moreover, as $\bar{d}_0$ increases (for given C_u), the mini-

mum value $(\theta_u)^{\min}$ of the undisturbed Shields parameter θ_u such that transport occurs within the whole cross section, increases.

The latter finding is more clearly described in Figure 11 where $(\theta_u^{\min}/\theta_c)$ is plotted directly as a function of the curvature ratio ν. Again, $\theta_u^{\min}$ increases as the curvature ratio ν increases. Notice that for relatively low values of ν, (say 0.1), $\theta_u^{\min}$ is not small, ranging about $(2-3)\theta_c$.

Finally Figure 12 shows typical shapes of the transverse bed profile for a partially transporting cross section with given C_u and θ_u and different values of the curvature ratio ν. As expected, when curvature increases (with given θ_u and C_u) the slope of the active portion of the bed increases; in other words, the incised part of the channel narrows and deepens.
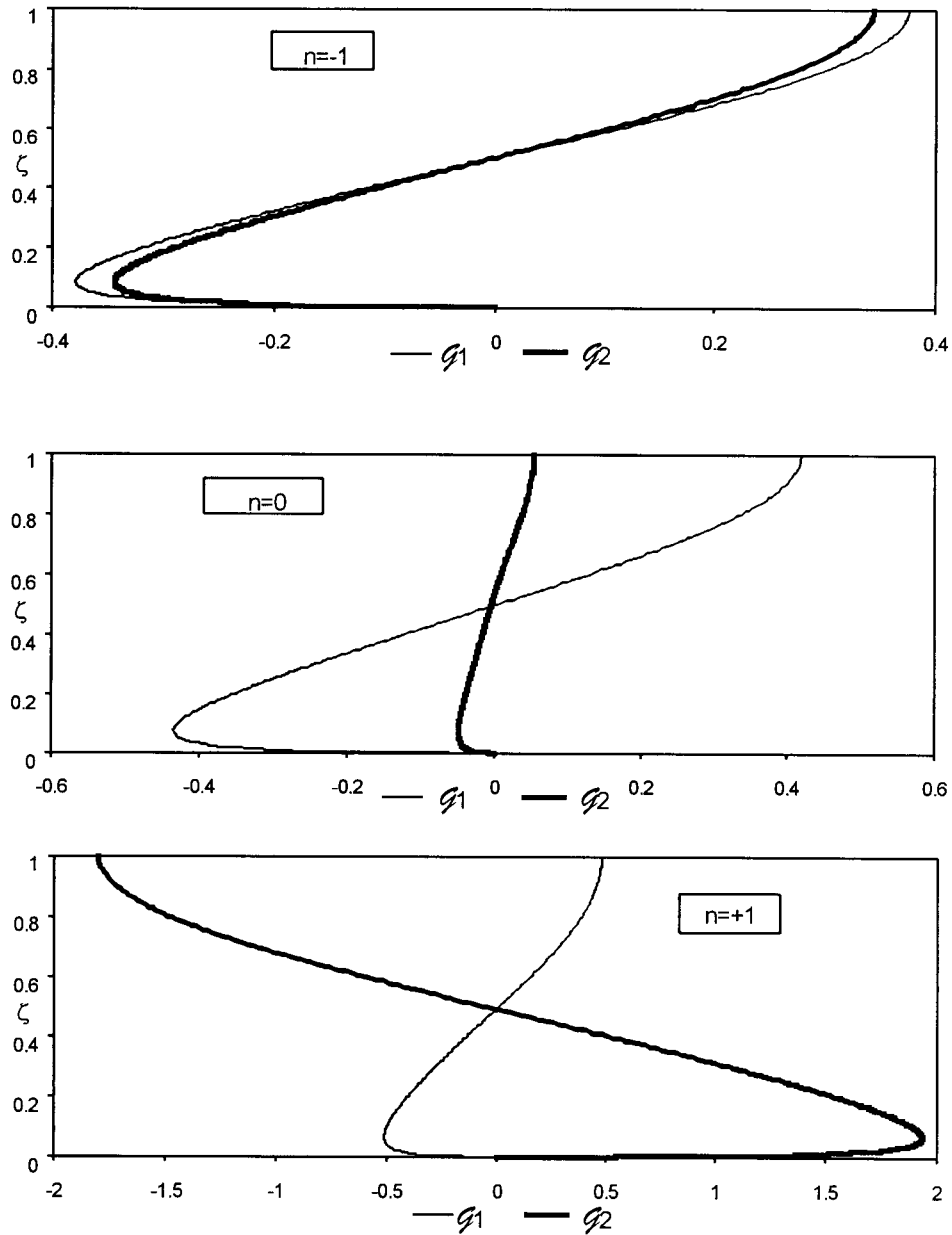
Figure 8. Typical vertical distribution of transverse velocity at $n = 0, 1, -1$ at leading order $\mathcal{G}_1$ (thin line) and first order $\mathcal{G}_2$ (thick line). Parameter values are $C_u = 0.004$, $\beta = 20$.

6. Conclusions

In the present work we have shown that finite amplitude deformations of the bottom profile do indeed occur in a constant curvature wide channel even for relatively small values of the curvature ratio ν. In fact, the analysis shows that the amplitude of deformations of the bottom profile scales by the parameter $\bar{d}_0$ defined by (34). Such a parameter typically attains values ranging to about 10. We have been able to account for the effect of such finite deformations both on the longitudinal flow and on the secondary flow: The former component is indeed found, at the leading order of approximation, to be proportional to the root of local flow depth, while the latter component turns out to scale by the 3/2 power of local flow depth.

Notice that such findings are in contrast with those of classical linear analyses where both the main and the secondary flow were found to be uniformly distributed in the cross section [see for instance *Seminara and Tubino*, 1989] at least at leading order.

A second result that emerged from the analysis is the need for a variation of channel slope to occur along the curved reach in order for the flow to be able to transport the sediment load coming from the straight reach. One may also interpret the above finding by stating that bed load transport rate is curvature dependent. In fact, one may calculate the dimensionless bed load transport rate Q_s^* in the curved channel as

$$Q_s = \frac{Q_s^*}{(2B^*)\sqrt{(s-1)gd_s^{*3}}} = \int_{-1}^{1} \phi[\theta(n)]\,dn \qquad (66)$$

where $\theta(n)$ is the local value of the Shields stress at location n within the curved reach. If channel slope in the curved reach
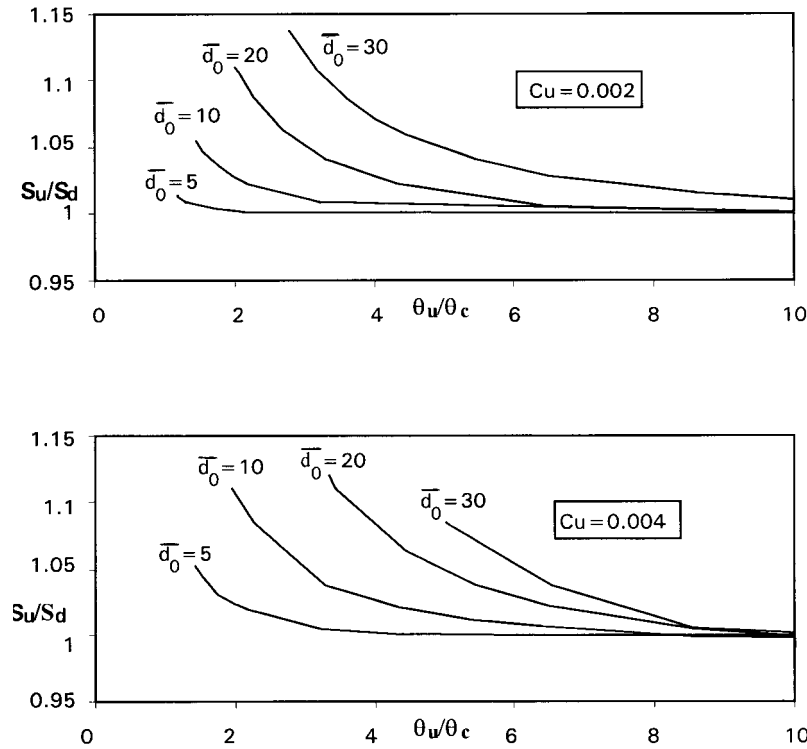
Figure 9. The ratio between the upstream value of bottom slope S_u and its downstream value S_d is plotted versus the ratio between the value of Shields stress in the straight reach and the critical value of Shield stress ($\theta_c = 0.047$) for given values of the scour parameter and the friction coefficient C_u.

were identical with the corresponding value for the straight reach, then $\theta(n)$ would simply be equal to $\theta_u D(n)$. Hence, for given values of the relevant parameters C_u and $\bar{d}_0$, one could calculate the transverse depth profile $D(n)$ and perform the integration in (66).

We have made this exercise and plotted the results thus obtained in Figure 13. It shows that the bed load transport rate that a constant curvature channel may accommodate without changing its slope relative to the slope of the incoming straight reach, differs from the bed load transport rate that a straight channel would allow under identical flow and sediment conditions. Such difference decreases slightly as the Shields parameter θ_u increases for given ν, while it increases as curvature increases for given value of θ_u.

Finally, the present approach has allowed us to evaluate the

conditions required for the whole cross section of the curved reach to be active. In fact, as curvature increases for given upstream conditions, the transverse slope of the channel increases such that the flow depth close to the inner bend may reduced to values so small as to not allow any sediment transport.

Exceeding such threshold conditions, say, a maximum value of ν for given θ_u (see Figure 11), implies that only a reduced portion of the cross section becomes active.

Notice that a linear theory, which predicts that the bed profile in a constant curvature channel is a straight line symmetrical with respect to the channel centerline, sharply over-
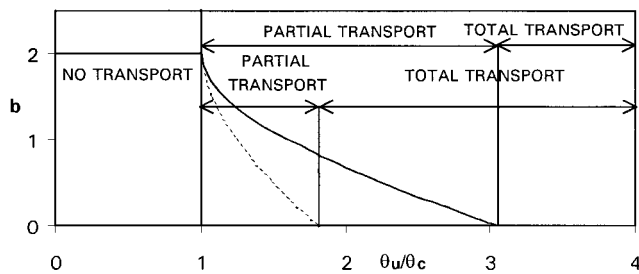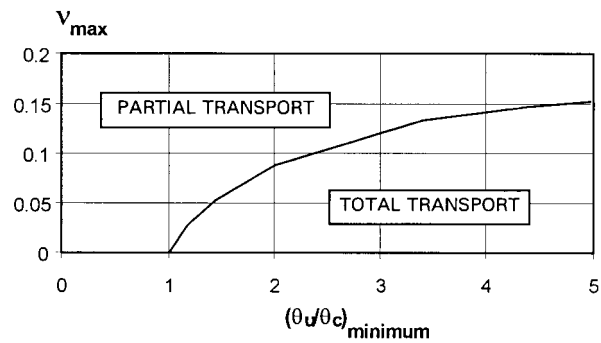

Figure 10. The length b of the inactive part for a partially transporting cross section is plotted versus the ratio between the value of Shields stress in the straight reach and the critical value of Shield stress θ_u/θ_c ($\theta_c = 0.047$) for given values of the scour parameter (dashed line, $\bar{d}_0 = 10$; solid line, $\bar{d}_0 = 20$) and for $C_u = 0.004$.

Figure 11. The ratio between the minimum value of Shields stress in the straight reach for the occurrence of total transport in the curved reach and the critical value of Shields stress ($\theta_c = 0.047$) is plotted versus ν. Notice that the curves referring to the values $C_u = 0.002$ and $C_u = 0.004$ are indistinguishable.
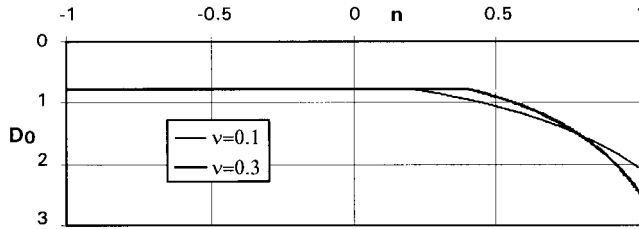
Figure 12. Typical bed profile of a partially transporting cross section for two different values of the parameter ν ($C_u = 0.004$, $S_u = 10^{-3}$).

estimates the flow depth at the inner bend. Hence linear theories would underestimate the threshold value of the curvature ratio ν for partial transport to occur.

The latter findings appear to be of particular interest in the context of gravel bed rivers where Shields stress remains relatively low.

In particular the restriction to uniform sediments has been recently removed by the present authors [see *Seminara et al.*, 1997] in the context of a theory formulated along the lines of the present approach. Relaxing the assumption of constant curvature is less straightforward and is an aim we are presently pursuing.

Notation

|	
A	constant, equal to 1.84.
b^*	length of the inactive part of the cross section.
B	constant, equal to -1.56.
B^*	half width of the channel.
C_u	friction coefficient of the uniform flow of discharge Q in a straight reach with slope S_u.
D	local value of dimensionless flow depth.
d_s^*	sediment diameter.
D_c^*	flow depth in the straight reach at the threshold conditions for sediment transport.
D_u^*	uniform flow depth in the straight reach.
$\bar{d}_0$	parameter, equal to $\nu(\theta_u)^{1/2}/C_u r$.
D_0, D_1	local dimensionless flow depth at the leading and first orders of approximation, respectively.
F_u	Froude number in the straight reach, equal to $U_u^*/(gD_u^*)^{1/2}$.
$\mathcal{F}_0, \mathcal{F}_1$	functions describing the vertical distributions of the dimensionless longitudinal component of velocity at the leading and first orders of approximation, respectively.
g	gravity.
$\mathcal{G}_1, \mathcal{G}_2$	functions describing the vertical distributions of the dimensionless transverse component of
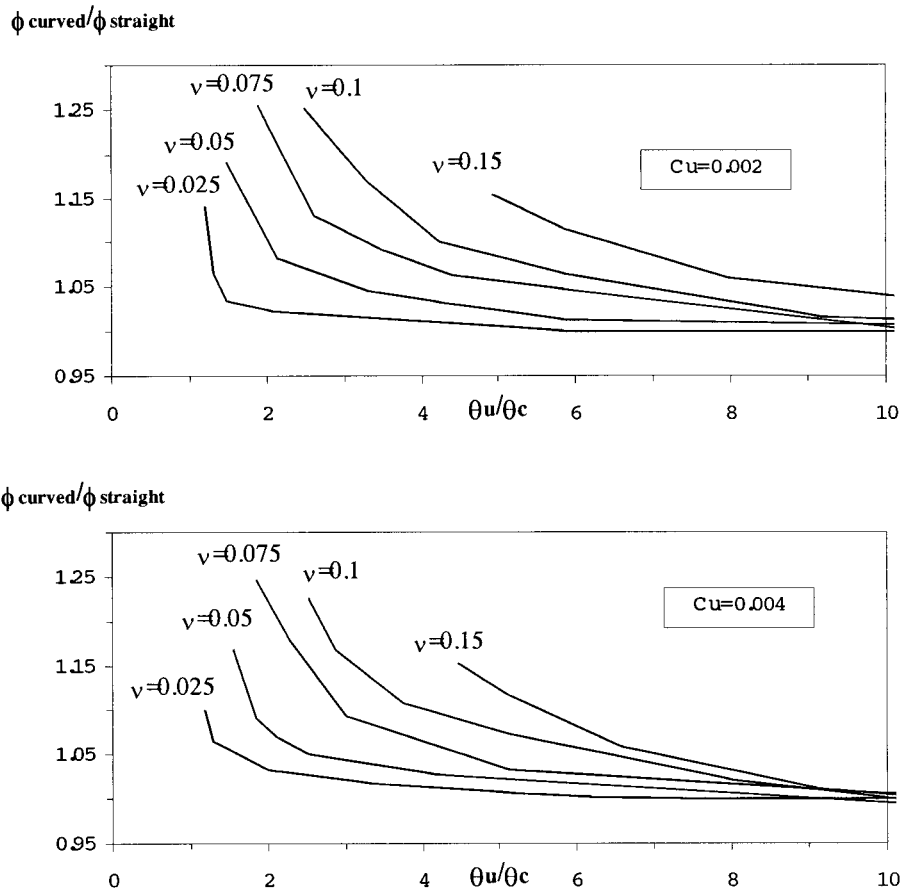
Figure 13. The ratio between the bed load transport rate in a constant curvature channel ϕ curved and the transport rate of the straight channel ϕ straight under identical flow and sediment conditions is plotted versus the Shields parameter θ_u of the straight channel for given values of the curvature ratio ν and the friction coefficient C_u.

            velocity at the leading and first orders of approximation, respectively.

h local value of the free surface elevation scaled by D_u^*.

h_s, h_n, h_z metric coefficients.

h_1, h_2 dimensionless definition of the local value of the free surface at the leading and first orders of approximation, respectively.

k von Karman's constant, equal to 0.4.

N vertical distribution of dimensionless eddy viscosity.

n^* transverse coordinate.

P^* mean pressure.

P_0, P_1 dimensionless pressure at the leading and first orders of approximation, respectively.

Q flow discharge.

q_n^* transverse component of the bed load discharge vector **q**.

r empirical constant, equal to 0.6.

r_o^* radius of curvature of channel axis.

s^* longitudinal coordinate.

S_d slope of the channel axis in the fully developed region of the bend.

S_u slope of the channel axis in the straight reach.

U^* local value of longitudinal velocity averaged over turbulence.

U_u^* average speed of the uniform flow of discharge Q in a straight reach with slope S_u.

U_0, U_1 local values of dimensionless longitudinal velocity at the leading and first order of approximation, respectively.

V^* local value of transverse velocity averaged over turbulence.

V_1, V_2 dimensionless transverse component of velocity at the first and second orders of approximation, respectively.

W^* local value of vertical velocity averaged over turbulence.

W_1, W_2 dimensionless vertical component of velocity at the first and second orders of approximation, respectively.

z^* nearly vertical coordinate.

z_0 local value of the conventional reference level for no-slip scaled by D_u^*.

β aspect ratio, equal to B^*/D_u^*.

δ small parameter, equal to $\nu/\beta(C_u)^{1/2}$.

θ local value of Shields stress.

θ_c critical value of Shields stress.

θ_u Shields stress in the straight reach.

η local value of the bed elevation scaled by D_u^*.

ν curvature ratio, equal to B^*/R_o^*.

ν_T^* local value of eddy viscosity.

ϱ water density.

ϱ_s sediment density.

τ^* shear stress at the bottom.

ϕ bed load function.

ϕ_u bed load function in the straight reach.

ζ normalized vertical coordinate.

References

Blondeaux, P., and G. Seminara, A unified bar-bend theory of river meanders, *J. Fluid Mech.*, *157*, 449–470, 1985.

Colombini, M., and M. Tubino, Finite amplitude multiple row bars: A fully nonlinear spectral solution, paper presented at Euromech 262, Sand Transport in Rivers, Estuaries and the Sea, Eur. Mech. Soc., Wallingford, U.K., June 26–29, 1990.

Dean, R. B., *Aero Rep. 74-11*, Imperial College, London, 1974.

De Vriend, H. J., A mathematical model of steady show in curved shallow channels, *J. Hydraul. Res.*, *15*(1), 37–54, 1977.

Ikeda, S., and G. Parker (Eds.), *River Meandering*, *Water Resour. Monogr.*, vol. 12, 485 pp., AGU, Washington, D. C., 1989.

Johannesson, H., and G. Parker, Secondary flow in mildly sinuous channel, *J. Hydraul. Eng.*, *115*(3), 289–308, 1989.

Kikkawa, H., S. Ikeda, and A. Kitagawa, Flow and bed topography in curved open channels, *J. Hydraul. Div. Am. Soc. Civ. Eng.*, *102*(HY9), 1326–1342, 1976.

Kovacs, A., and G. Parker, A new vectorial bedload formulation and its application to the time evolution of straight river channels, *J. Fluid Mech.*, *267*, 153–183, 1994.

Nelson, J. M., and A. D. Smith, Flow in meandering channels with natural topography, in *River Meandering*, *Water Resour. Monogr.*, vol. 12, edited by S. Ikeda and G. Parker, pp. 69–102, AGU, Washington, D. C., 1989.

Parker, G., Surface-based bedload transport relation for gravel rivers, *J. Hydraul. Res.*, *20*(4), 417–436, 1990.

Rozovskij, I. L., Flow of water in bends of open channels, *Acad. Sci. Ukranian SSR*, 1957.

Seminara, G., and M. Tubino, Alternate bars and meandering: Free, forced and mixed interactions, in *River Meandering*, *Water Resour. Monogr.*, vol. 12, edited by S. Ikeda and G. Parker, pp. 267–320, AGU, Washington, D. C., 1989.

Seminara, G., and M. Tubino, Weakly nonlinear theory of regular meanders, *J. Fluid Mech.*, *244*, 257, 1992.

Seminara, G., L. Solari, and M. Tubino, Finite amplitude scour and grain sorting in wide channel bends, paper presented at 27th Congress, Int. Assoc. for Hydraul. Res., San Francisco, Calif., 1997.

Shimizu, Y., H. Yamaguchi, and T. Itakura, Three-dimensional computation of flow and bed deformation, *J. Hydraul. Eng.*, *116*(9), 1090–1108, 1990.

Smith, J. D., and S. R. McLean, A model for flow in meandering streams, *Water Resour. Res.*, *20*(9), 1301–1315, 1984.

Struiksma, N., K. W. Olesen, C. Flokstra, and H. J. de Vriend, Bed deformation in curved alluvial channels, *J. Hydraul. Res.*, *23*(1), 57–79, 1986.

Talmon, A. M., N. Struiksma, and M. C. L. M. Van Mierlo, Laboratory measurements of the direction of sediment transport on transverse alluvial-bed slopes, *J. Hydraul. Res.*, *33*(4), 519–534, 1995.

Tubino, M., and G. Seminara, Free-forced interactions in developing meanders and suppression of free bars, *J. Fluid Mech.*, *214*, 131–159, 1990.

U.S. Army Corps of Engineering, *Eng. Manual 1110-2-1601*, 1991.

G. Seminara and L. Solari, Istituto di Idraulica, Università di Genova, via Montallegro, 1, 16145 Genova, Italy. (e-mail: sem@idra. unige.it)